POLYMERS

Catalyst-controlled stereoselective cationic polymerization of vinyl ethers

A. J. Teator and F. A. Leibfarth*

The tacticity of vinyl polymers has a profound effect on their physical properties. Despite the well-developed stereoselective methods for the polymerization of propylene and other nonpolar α-olefins, stereoselective polymerization of polar vinyl monomers has proven more challenging. We have designed chiral counterions that systematically bias the reactivity and chain-end stereochemical environment during cationic polymerization. This approach overrides conventional chain-end stereochemical bias to achieve catalyst-controlled stereoselective polymerization. We demonstrate that this method is general to vinyl ether substrates, providing access to a range of isotactic poly(vinyl ether)s with high degrees of isotacticity. The obtained materials display the tensile properties of commercial polyolefins but adhere more strongly to polar substrates by an order of magnitude, indicating their promise for next-generation engineering applications.

The tacticity of vinyl polymers is intimately linked to their resultant material properties. The desirable thermomechanical properties of isotactic polypropylene (*i*PP), which is produced at a scale exceeding 50 million metric tons annually (*1*), are a direct consequence of its stereoregular microstructure. In the coordination-insertion polymerizations that produce *i*PP and other isotactic poly(α-olefin)s, the chiral ligand environment of an organometallic complex biases facial addition of incoming monomers to the propagating polymer chain end (Fig. 1A). However, monomers containing polar functionality lead to catalyst poisoning and are limited to polymerizations mediated by complex chiral metallocenium catalysts (*2*, *3*). These methods typically proceed through a coordination-addition mechanism that necessitates an enolizable monomer and thus are not generally applicable (*4*). Late transition metal catalysts have been developed to circumvent such limitations, but these typically have insufficient catalytic activity to introduce polar co-monomers into polyolefins at a scale necessary for high-performance engineering applications (*5*–*9*).

Because of the limitations of coordination-insertion approaches, the polymerization of polar vinyl monomers is typically conducted by radical or ionic mechanisms. These methods proceed via achiral propagating chain ends that provide no obvious mode for biasing the facial addition of subsequent monomers (Fig. 1B). The development of general methods for the stereoselective polymerization of polar monomers would expand the diversity of properties accessible from otherwise readily available starting materials. The few reported stereoselective radical and ionic polymerizations rely on chain-end control, whereby the stereochemistry of the last enchained monomer influences the stereochemistry of subsequent monomer addition (*10*, *11*). In contrast to the catalyst-controlled coordination-insertion polymerization of α-olefins, approaches that rely on chain-end control are not general to monomer class. A fundamentally different approach for the stereoselective polymerization of polar monomers is to design a chiral counterion that mediates the facial addition of polar vinyl monomers to an ionic chain end.

We identified the cationic polymerization of vinyl ethers as a high-value target to exemplify such a catalyst-controlled approach. Poly(vinyl ether)s (PVEs) feature a polar ether functionality in each repeat unit, are derived from an inexpensive and underused feedstock, and are rarely used commercially because of their amorphous properties at room temperature (*12*). The lack of a general, catalyst-controlled stereoselective vinyl ether polymerization has precluded exploration of semicrystalline PVEs as a class of viable polar polyolefin analogs. Previous approaches toward stereoselective vinyl ether polymerizations have exclusively relied on chain-end control to dictate facial addition to the propagating oxocarbenium ion, which has provided access to isotactic PVEs in specific cases but is not general to alkyl vinyl ether monomers as a class (*13*–*19*). For example, the state-of-the-art method uses a phenoxide-ligated titanium complex to achieve 92% *meso* diads (% *m*) in the polymerization of *iso*-butyl vinyl ether (*i*BVE) (*20*). This method, however, is highly sensitive to monomer structure and achieved only 76% *m* and 64% *m* in the case of *n*-butyl (BVE) and ethyl vinyl ether (EVE), respectively. Extensive structural modifications of the phenoxide ligand resulted in diminished stereoselectivity, and the ultimate origin of stereoinduction resulted from an undetermined interplay of monomer and catalyst steric interactions. This high substrate specificity is common for stereoselective polymerizations governed by chain-end control and exemplifies the challenges of designing general catalytic methods using this approach (*21*).

Drawing inspiration from asymmetric ion-pairing catalysis (*22*), we chose to leverage the modularity of 1,1′-bi-2-naphthol (BINOL)–based phosphoric acids in order to systematically tune the reactivity and chain-end interactions of chiral counterions (Fig. 1C). Considering that BINOL-derived chiral phosphoric acids such as **3a** have been successfully used to mediate enantioselective additions to oxocarbenium reactive intermediates, we exposed *i*BVE to chiral acid **3a** (*23*, *24*). No polymerization was observed, likely on account of the stability of the formed Markovnikov addition product (Fig. 2A, **1**). For this reason, we investigated Lewis acid additives that have previously been shown to promote ionization (**2**) and enable cationic polymerization initiated by weak Brønsted acids (*25*). The addition of $TiCl_4$ (0.2 equivalents relative to **3a**) to a mixture of *i*BVE and **3a** at −78°C resulted in polymerization to afford poly(*i*BVE). Integration of the ^{13}C nuclear magnetic resonance (NMR) backbone methylene resonances (δ 39 to 42 ppm, $CDCl_3$) revealed 82% *m*, a substantial improvement over an analogous control reaction that used HCl in place of **3a** (73% *m*). We hypothesized that this increase was a direct result of the formation of a chiral anion, likely composed of **3a** and $TiCl_4$.

To evaluate the effect of the phosphoric acid structure on the polymerization, we prepared a library of phosphoric acids featuring various steric and electronic environments (Fig. 2B). With the exception of the sterically hindered **3b** TRIP [3,3′-bis(2,4,6-triisopropylphenyl)-1,1′-binaphthyl-2,2′-diyl hydrogenphosphate] (*26*, *27*), all phosphoric acid derivatives produced polymer when subjected to the reaction conditions described above. Replacing the 3,5-bis(trifluoromethyl) phenyl group in **3a** with a phenyl substituent (**3c**) resulted in a material with decreased isotacticity (78% *m*). Increasing the number of fused rings (i.e., **3d** and **3e**) or adjusting the steric environment by incorporating mesityl groups (**3f**) produced materials with inferior isotacticity; however, the introduction of perfluorophenyl groups (**3g**) resulted in a degree of stereocontrol approaching that observed with **1**. The addition of a trifluoromethyl group at the *para* position (**3h**) had deleterious effects on stereocontrol, which suggests that the 3,5-substitution pattern of **3a** may be essential for obtaining high stereoselectivity.

We hypothesized that a Ti complex (**5**), with **3a** serving as a ligand, is ultimately responsible for stereoselectivity (Fig. 3A). To confirm this hypothesis, we first mixed **3a** with $TiCl_4$ prior to the addition of monomer and observed an increase in stereoselectivity from 83% to 87% *m*. We further hypothesized that liberated HCl formed upon ligation of **3a** to $TiCl_4$ acted as an endogenous initiator to form **4**, which was confirmed in a series of control experiments (see table S2) (*28*). A subsequent evaluation of Lewis

Department of Chemistry, University of North Carolina, Chapel Hill, NC 27599, USA.
*Corresponding author. Email: frankl@email.unc.edu

acid complexes led to the discovery that $TiCl_4(THF)_2$ (THF, tetrahydrofuran) was the optimal Lewis acid to obtain high stereoselectivity (Fig. 3B), achieving 91% *m* poly(*i*BVE) (see table S3). Further optimization of reaction conditions (i.e., [*i*BVE]$_0$ and Lewis basic additives) produced increases in stereocontrol that resulted in poly(*i*BVE) with 93.0 ± 0.2% *m* (Fig. 3C and table S5). Additionally, analysis of triad tacticity using Markovian statistics suggests an overwhelming preference for catalyst control, particularly when compared to a control reaction performed solely with $TiCl_4$ (see table S4) (*29*, *30*). An initial kinetic analysis suggested behavior consistent with chain-growth polymerization, with high–molecular

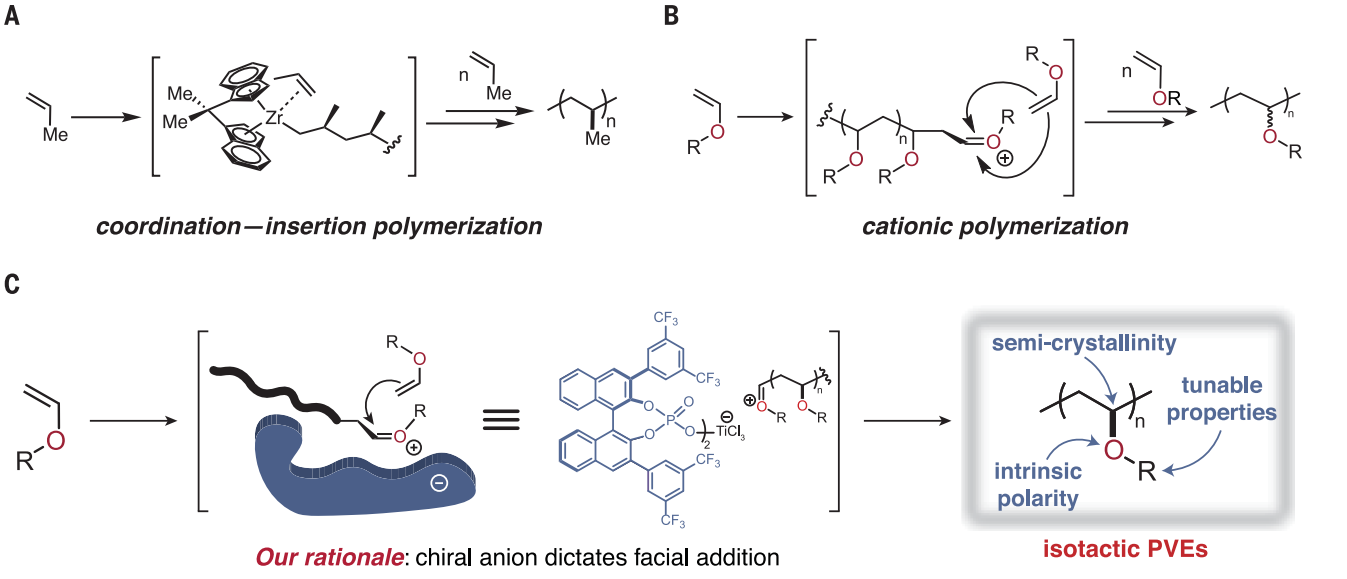

Fig. 1. Designing a stereoselective cationic polymerization. (**A**) The chiral ligand environment in coordination-insertion polymerizations enables stereoselective monomer enchainment by directing facial addition at the propagating polymer chain end. Polar monomers are typically not compatible with this mechanism because of catalyst poisoning. Me, methyl. (**B**) The achiral chain end in the cationic polymerizations of vinyl ethers provides no inherent mode for stereoinduction. Monomer addition occurs at either face of the oxocarbenium ion. (**C**) Our catalyst-controlled approach to stereoselective cationic polymerization relies on a chiral, BINOL-based counterion to bias the stereochemistry of monomer enchainment. The resultant isotactic PVEs are semicrystalline thermoplastics with intrinsic polarity.

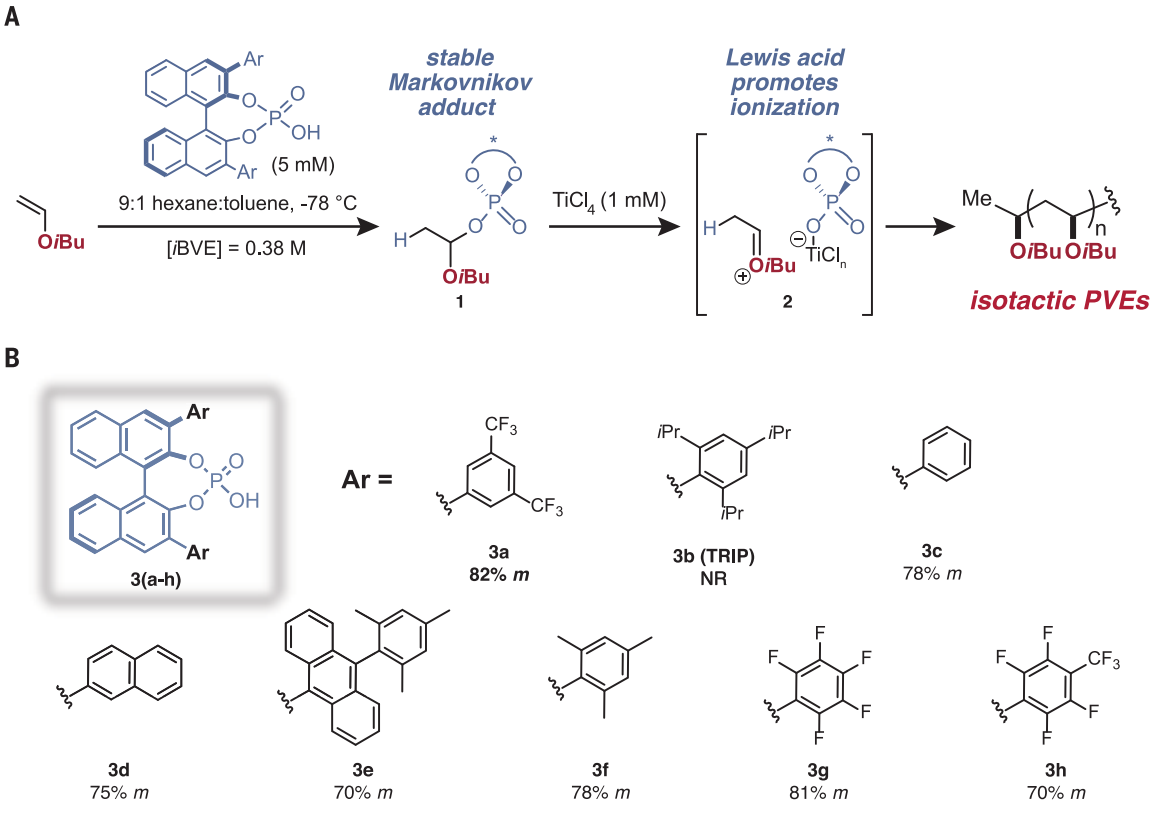

Fig. 2. Initial optimization of reaction conditions. (**A**) Reaction scheme depicting Lewis acid–assisted polymerization of *i*BVE using BINOL-based phosphoric acids. *i*Bu, isobutyl; Ar, aryl. (**B**) Evaluation of the influence of phosphoric acid aryl substituents on stereocontrol during *i*BVE polymerization. *i*Pr, isopropyl; NR, no reaction.

weight materials with dispersity values close to 2 formed at moderate conversions.

To probe the solution structure of the catalyst responsible for stereoselectivity, we varied the stoichiometry of **3a** relative to $TiCl_4(THF)_2$. Increases in % *m* were observed when transitioning from zero to one to two equivalents of **3a** relative to $TiCl_4(THF)_2$. The addition of more than two equivalents of **3a** relative to Lewis acid resulted in further small increases in stereocontrol. These experimental observations, in combination with low-temperature ^{31}P NMR data, indicated an equilibrium process whereby the Ti complex responsible for stereoselectivity is ligated by two phosphoric acids (**5**), and excess **3a** serves to drive formation of the desired adduct (see table S6 and fig. S32).

Having demonstrated the stereoselective polymerization of *i*BVE using a synergistic combination of **3a** and $TiCl_4(THF)_2$, we sought to probe the substrate scope of this methodology for alkyl vinyl ether monomers. As shown in Fig. 3D, stereoselective polymerization was realized without altering the optimized reaction conditions to afford isotactic PVEs bearing a variety of alkyl substituents. The greatest degree of stereoinduction was observed for monomers with linear alkyl substituents, such as in EVE (92.0 ± 0.1% *m*), *n*-propyl vinyl ether (PrVE, 92.2 ± 0.1% *m*), and BVE (93.2 ± 0.1% *m*). Branched alkyl substituents, such as in *i*BVE (93.0 ± 0.2% *m*) and isopropyl vinyl ether (*i*PVE, 87.6 ± 0.4% *m*), were also well tolerated.

As illustrated in Fig. 3E, our approach produced solid, semicrystalline PVEs, whereas the atactic materials produced by chain-end control remain amorphous liquids. We first investigated thermal stability using thermogravimetric analysis (TGA). All of the obtained materials were thermally robust, with decomposition onset temperatures (T_d, temperature at 5% weight loss) greater than 325°C. Isotactic PVEs were further evaluated using differential scanning calorimetry (DSC), which revealed semicrystalline polymers with a wide range of glass transition temperatures T_g and melting points T_m (Fig. 4A). All of the obtained isotactic PVEs featured T_g values well below room temperature, with limits defined by poly(BVE) (–53°C) and poly(*i*PVE) (–14°C). Isotactic PVEs with linear side chains (i.e., ethyl, propyl, butyl) featured single melting transitions that ranged from 65° to 76°C, whereas isotactic PVEs with branched side chains (i.e., isopropyl, isobutyl) featured relatively high T_m values that manifested as two separate first-order transitions and ranged from 138° to 152°C. The appearance of multiple melting transitions is characteristic of many semicrystalline homopolymers and is likely related to melting of an initial crystal morphology and subsequent recrystallization (fig. S34) (*31*).

Scaling up the stereoselective polymerization to achieve multigram quantities of isotactic PVEs was straightforward and provided sufficient material for further structure-property evaluations. The large thermal processing window (above the T_m and below the T_d) of isotactic PVEs enabled us to melt-press films of the material. The crystalline nature of the isotactic PVE films was confirmed by wide-angle x-ray diffraction (WAXD; Fig. 4B), which revealed d-spacing (9.8 Å) that was predictably larger than that measured in *i*PP (6.4 Å). We next explored the mechanical

Fig. 3. Optimization, monomer screen, and representative isotactic PVEs. (**A**) The proposed ionization mechanism of Lewis acid (LA) complex **5**. (**B**) Optimization of polymerization conditions to achieve high poly(*i*BVE) tacticity. Conditions: **3a** (5 mM), LA (1 mM), *i*BVE, additive, 8:2 hexane:toluene, –78°C. *Đ*, dispersity. (**C**) Differences in salient ^{13}C NMR resonances observed in atactic and isotactic PVEs. (**D**) Monomer scope demonstrating generality of the methodology. Et, ethyl. (**E**) Visual representation (photo) highlighting difference between poly(*i*BVE) samples that are 69% *m* and 91% *m*.

A

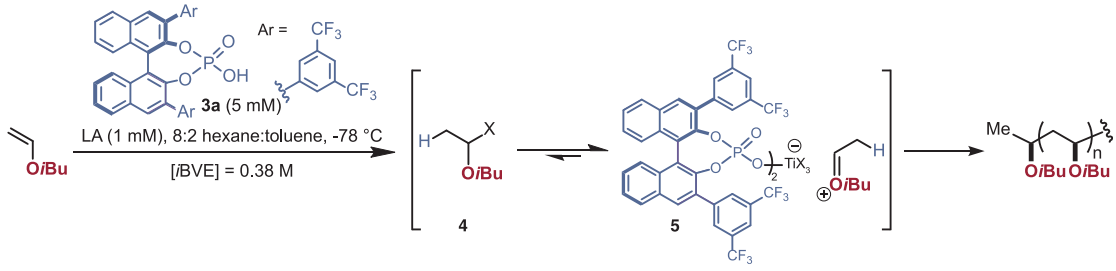

B

LA	[*i*BVE] (M)	additive	M_n (kg mol^{-1})	*Đ*	*m* (%)
$TiCl_4$	0.38	none	86	1.9	87
$TiBr_4$	0.38	none	106	3.2	87
$ZrCl_4(THF)_2$	0.38	none	44	2.2	81
$TiCl_4(THF)_2$	0.38	none	70	1.4	91
$TiCl_4(THF)_2$	0.38	THF (10 mM)	69	2.4	92
$TiCl_4(THF)_2$	0.10	THF (10 mM)	25	1.6	93

C

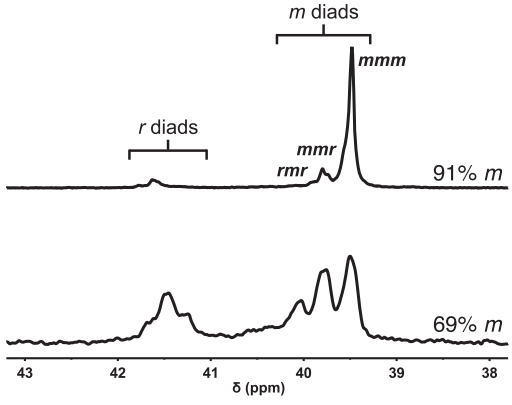

D

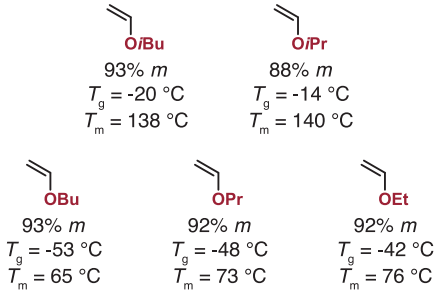

E

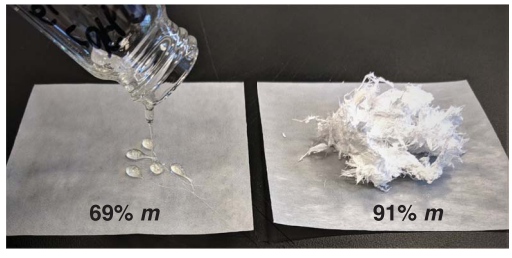

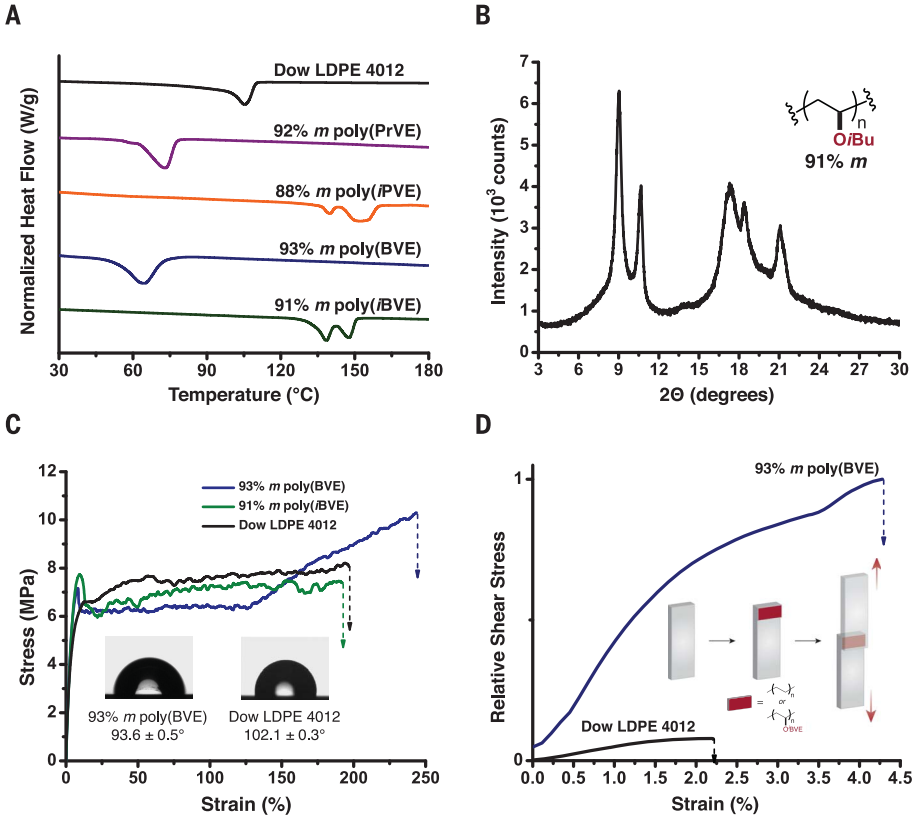

Fig. 4. Evaluation of thermomechanical and surface properties. (**A**) DSC second-heating-scan curves (10°C/min) for various isotactic PVEs and Dow LDPE 4012. (**B**) Representative WAXD pattern of a melt-pressed 91% *m* poly(*i*BVE) film. (**C**) Overlay of stress-strain curves for 93% *m* poly(BVE), 91% *m* poly(*i*BVE), and Dow LDPE 4012 measured by tensile testing (5 mm/min, room temperature, break point indicated by dashed arrow). The inset is a visual representation (photo) of the static contact angle of water on melt-pressed films of 93% *m* poly(BVE) and Dow LDPE 4012. (**D**) Relative shear stress–strain curves for poly(BVE) and Dow LDPE 4012 single-lap joints measured by tensile testing (5 mm/min, room temperature). The inset illustrates the lap-shear experiment.

properties of these materials by dynamic mechanical analysis in linear film tension mode. Tensile testing of dog bone–shaped specimens cut from melt-pressed films of poly(BVE) and poly(*i*BVE) yielded stress-strain curves that showed plastic deformation behavior typical of semicrystalline thermoplastics (Fig. 4C). A similar Young's modulus (E) was observed for both poly(BVE) (E = 160 ± 30 MPa) and poly(*i*BVE) (E = 200 ± 20 MPa); the yield strength (σ_y) of poly(*i*BVE) (σ_y = 8.4 ± 0.5 MPa) was slightly higher than that of poly(BVE) (σ_y = 6.5 ± 0.5 MPa). The elongation at break value of poly(BVE) (ε_B = 260 ± 20%) was relatively large relative to poly(*i*BVE) (ε_B = 170 ± 20%). Strain stiffening was observed in films of poly(BVE), which resulted in a greater tensile strength (σ_b = 9.8 ± 0.7 MPa) than that measured for poly(*i*BVE) (σ_b = 8.2 ± 0.5 MPa). Overall, the critical thermomechanical properties of both poly(BVE) and poly(*i*BVE) compare well to commercial polyolefins, such as the low-density polyethylene Dow LDPE 4012 (T_m = 105°C, E = 280 ± 40 MPa, σ_y = 8 ± 1 MPa, σ_b = 10 ± 2 MPa).

Building on these results, subsequent efforts were directed toward the investigation of surface and adhesive properties of isotactic PVEs. In addition to having thermomechanical properties commensurate with that of commercial polyolefin materials (i.e., LDPE), we expected isotactic PVEs to exhibit significantly different surface properties due to their intrinsic polarity. Initially, the static contact angle of water on films of poly(BVE) was measured to establish the relative hydrophilicity of the isotactic polymers (Fig. 4C). Poly(BVE) displayed a contact angle of 93.6° ± 0.5°, substantially lower than that observed for Dow LDPE 4012 (102.1° ± 0.3°). On this basis, we reasoned that poly(BVE) should display superior adhesion to polar surfaces (i.e., glass) relative to polyolefin materials. To test this hypothesis, we prepared a single-lap joint between two glass slides, using poly(BVE) or Dow LDPE 4012, and subjected it to lap shear analysis (Fig. 4D). Poly(BVE) demonstrated stronger adhesion to glass than did the Dow LDPE material by more than an order of magnitude, with apparent lap shear strengths of 1600 ± 100 MPa and 130 ± 20 MPa, respectively. Furthermore, the strong adhesion of isotactic PVEs to glass substrates resulted in cohesive failure, whereas adhesive failure was consistently observed for polyolefin-bonded lap joints (fig. S33). Collectively, these results show that the intrinsic polarity of vinyl ethers has a fundamental impact on the adhesion of isotactic PVEs to polar surfaces relative to hydrophobic polyolefins.

We anticipate that the concept of chiral counterion catalysis to control polymer tacticity will extend to a range of stereoselective polymerizations, while the continued development and structure-property evaluation of isotactic PVEs will enhance polar thermoplastics for next-generation engineering applications.

REFERENCES AND NOTES

1. V. Busico, *Adv. Polym. Sci.* **257**, 37–58 (2013).
2. S. D. Ittel, L. K. Johnson, M. Brookhart, *Chem. Rev.* **100**, 1169–1204 (2000).
3. S. Ito, K. Nozaki, *Chem. Rec.* **10**, 315–325 (2010).
4. E. Y.-X. Chen, *Chem. Rev.* **109**, 5157–5214 (2009).
5. G. J. Domski, J. M. Rose, G. W. Coates, A. D. Bolig, M. Brookhart, *Prog. Polym. Sci.* **32**, 30–92 (2007).
6. B. P. Carrow, K. Nozaki, *Macromolecules* **47**, 2541–2555 (2014).
7. A. Nakamura *et al.*, *Acc. Chem. Res.* **46**, 1438–1449 (2013).
8. W. Zhang *et al.*, *J. Am. Chem. Soc.* **140**, 8841–8850 (2018).
9. N. M. G. Franssen, J. N. H. Reek, B. de Bruin, *Chem. Soc. Rev.* **42**, 5809–5832 (2013).
10. G. W. Coates, *Chem. Rev.* **100**, 1223–1252 (2000).
11. Y. Okamoto, T. Nakano, *Chem. Rev.* **94**, 349–372 (1994).
12. G. Schröder, in *Ullmann's Encyclopedia of Industrial Chemistry* (Wiley, 2000), vol. 28, pp. 481–485.
13. L. Fishbein, B. F. Crowe, *Makromol. Chem.* **48**, 221–228 (1961).
14. G. Natta *et al.*, *Macromolecules* **2**, 311–315 (1969).
15. C. E. Schildknecht, C. H. Lee, K. P. Long, *Polym. Eng. Sci.* **7**, 257–263 (1967).
16. S. Aoshima, Y. Ito, E. Kobayashi, *Polym. J.* **25**, 1161–1168 (1993).
17. H. Ohgi, T. Sato, *Polymer* **43**, 3829–3836 (2002).
18. T. Kawaguchi, F. Sanda, T. Masuda, *J. Polym. Sci. A* **40**, 3938–3943 (2002).
19. M. Ouchi, M. Sueoka, M. Kamigaito, M. Sawamoto, *J. Polym. Sci. A* **39**, 1067–1074 (2001).
20. M. Ouchi, M. Kamigaito, M. Sawamoto, *Macromolecules* **32**, 6407–6411 (1999).
21. M. Ouchi, M. Kamigaito, M. Sawamoto, *J. Polym. Sci. A* **39**, 1060–1066 (2001).
22. K. Brak, E. N. Jacobsen, *Angew. Chem. Int. Ed.* **52**, 534–561 (2013).
23. J. H. Tay *et al.*, *J. Am. Chem. Soc.* **139**, 8570–8578 (2017).
24. Z. Sun, G. A. Winschel, P. M. Zimmerman, P. Nagorny, *Angew. Chem. Int. Ed.* **53**, 11194–11198 (2014).
25. M. Kamigaito, Y. Maeda, M. Sawamoto, T. Higashimura, *Macromolecules* **26**, 1643–1649 (1993).
26. T. Akiyama, Y. Tamura, J. Itoh, H. Morita, K. Fuchibe, *Synlett* **2006**, 141–143 (2006).
27. S. Hoffmann, M. Nicoletti, B. List, *J. Am. Chem. Soc.* **128**, 13074–13075 (2006).
28. S. Aoshima, S. Kanaoka, *Chem. Rev.* **109**, 5245–5287 (2009).
29. Y. Doi, T. Asakura, *Makromol. Chem.* **176**, 507–509 (1975).
30. J. A. Byers, J. E. Bercaw, *Proc. Natl. Acad. Sci. U.S.A.* **103**, 15303–15308 (2006).
31. R. Paukkeri, A. Lehtinen, *Polymer* **34**, 4083–4088 (1993).

ACKNOWLEDGMENTS

This work was performed in part at the Mass Spectrometry Core Laboratory at UNC Chapel Hill (NSF CHE-1726291) and the Chapel Hill Analytical and Nanofabrication Laboratory (CHANL, NSF ECCS-1542015). We thank Dow Chemical for providing a sample of LDPE 4012. **Funding:** Supported by Army Research Office grant W911NF1810084. **Author contributions:** A.J.T. and F.A.L. designed the experiments; A.J.T. conducted and analyzed the experiments; A.J.T. and F.A.L. prepared the manuscript. **Competing interests:** A.J.T. and F.A.L. are listed as inventors on a provisional patent application describing the stereoregular polymerization of vinyl ether monomers (62/719,240). **Data and materials availability:** Experimental and characterization data are provided in the supplementary materials.

SUPPLEMENTARY MATERIALS

www.sciencemag.org/content/363/6434/1439/suppl/DC1
Materials and Methods
Supplementary Text
Figs. S1 to S34
Tables S1 to S6
References (*32*–*41*)

24 November 2018; accepted 7 February 2019
10.1126/science.aaw1703

Catalyst-controlled stereoselective cationic polymerization of vinyl ethers

A. J. Teator and F. A. Leibfarth

Science **363** (6434), 1439-1443.
DOI: 10.1126/science.aaw1703

The right hand lines up vinyl ethers

Well-optimized catalysts produce vast quantities of isotactic polypropylene, in which the side chains all face the same way. Add an oxygen into the monomer, though, and that degree of uniformity becomes harder to enforce. Teator and Leibfarth report a general protocol to polymerize a variety of such vinyl ethers isotactically (see the Perspective by Foster and O'Reilly). They rely on a chiral phosphoric acid in combination with a titanium Lewis acid to bias the monomer orientation during cationic polymerization. The resulting polymers show promising adhesive properties.

Science, this issue p. 1439; see also p. 1394